Evaluation of turbulent models in sudden expansion analysis at High Reynolds numbers

ABBAS MANSOORI* and **MOHAMMAD REZA BAZARGAN-LARI****
* Department of Civil Engineering, post-graduate school, Islamic Azad University-South Tehran branch, Tehran, Iran

** Ph.D. Candidate of Islamic Azad University-Science and Research Branch and Faculty of Civil Engineering Dept., Islamic Azad University-East Tehran Branch., Tehran, Iran.

Abstract: Using abrupt expansion as an energy dissipater in bottom outlet of dams may have unfavorable effects on dam safety due to cavitation. Domain and intensity of cavitation, depends on magnitude and location of negative pressure. Therefore predicting the extent and intensity of negative pressure plays an important role in detection of cavitation. On the other hand, there is no globally accepted turbulence model to predict negative pressure. In this paper an experimental investigation has been performed to determine the variation of pressure. Different turbulent models were ranked through the comparison of analytical and experimental results. It was found that the Realizable $k-\varepsilon$ model has better prediction with respect to the others.

Key-Words: Computational Fluid Dynamics, Turbulent models, sudden expansion, wall-pressure, energy dissipation, cavitation.

1 Introduction

The axisymmetric sudden expansion is a kind of flow separation in which complex turbulent flow may occur. In many practical engineering applications such as conduit flow systems, petroleum industries, air-condition ducts and fluidic devices, etc. this kind of flow may be encountered.
The safe use of large conduit expansion as an energy dissipater in bottom outlet of dams led the writers to investigate the location and magnitude of Maximum Negative Pressure (MNP) which can be used as a parameter for a proper selection of turbulent model.
Although there are significant number of experimental and theoretical investigations on turbulent flows through axisymmetric sudden expansion, literature is surprisingly limited on prediction of magnitude and location of MNP. Chaturvedi (Chaturvedi 1963) was one of the first researchers who investigated the jet flow characteristics of axisymmetric expansions. He concluded that due to the complex nature of the phenomenon, it is impossible to express the results and details of the jet flow characteristics in simple mathematical formulations. Rouse H., and Jezdinsky (Rouse H. and Jezdinsky 1966), investigated both the energy loss and limiting conditions of cavitations experimentally. Johnson (Johnson 1976) divided the jet flow in suddenly expanded pipe into recirculating, reattaching and redeveloping zones. Poole and Escudier (Poole and Escudier 2004) investigated the variation of wall pressure for both Newtonian (water) and non-Newtonian fluid flow due to sudden expansion. Other methods such as pitot tubes (Chaturvedi 1963 and Mansoori 1988), dye injection; (Back and Roschke1972), Laser Doppler Anemometry; (Moon and Rudiger 1977), (Szczepura 1985), (Stieglmeirer et al. 1989), (Sulliva and Glauser 1990) and Hot-wire anemometry are also used to study the axisymmetric confined jet in sudden expansion experimentally.
Since experimental investigations of sudden expansion are expensive and time consuming, numerical analysis are growing rapidly. Among these numerical methods the Reynolds Averaged Navier-Stokes (RANS) method is the most popular mathematical model which is used in different computational fluid dynamics (CFD) based codes. In each CFD based modeling, the first question is that: "which available turbulent model is proper to use for a specific case?". The purpose of this paper is to answer the mentioned question by modeling an axisymmetric sudden expansion jet in FLUENT V6. In other words this paper is aimed to find and present a proper turbulent model (among various available ones) which has the best correlation with experimental results.

2 Development of measuring system

Please, leave two blank lines between successive sections as here.

There are two main factors which must be considered in the design of any turbulence measuring device:

1-Device should be smaller than the micro scale of turbulence (i.e. in this case the bore diameter of the Pitot-Tube).

2-It has flat response to all frequencies lower than some characteristic velocity divided by the micro scale.

With a total head tube however, the frequency response is proportional to the tube diameter, therefore the true requirements are in opposition to each other.

The accuracy of the turbulent data depends upon five factors as follows:

a) Relative intensity of turbulence.
b) Frequency response relative to the spectral distribution of turbulent energy.
c) Size of probe relative to the scale of the turbulence.
d) Effective center of the probe, which is shifted by the influence of the higher velocity region.
e) Creation of asymmetrical flow around the tube near the wall.

As measurement are generally limited to an Eulerian frame of reference, it is difficult to distinguish between a truly temporal change in a flow quantity and a pseudo-temporal change due to a spatially varying disturbance convicted past the fixed probe. It is essential that there be a proper balance between the spatial resolution and temporal response of the instrumentation.

In an Eularian frame of reference, conservation of mass and momentum yields:

$$\frac{\partial u_i}{\partial x_i} = 0 \text{ (In tensor notation)} \qquad (1)$$

$$\frac{Du}{Dt} = x_i + \frac{\partial \tau_{ji}}{\partial x_j} \qquad (2)$$

$$\frac{D}{Dt} = \frac{\partial}{\partial t} + u_i\left(\frac{\partial}{\partial x_i}\right) \qquad (3)$$

Where x_i are the components of the body forces field. In inviscid frictionless flow the only term in the stress tensor τ_{ji} is the pressure P. Then,

$$\frac{Du_i}{Dt} = x_i + \frac{\partial p}{\partial x_i} \qquad (4)$$

Where P is positive for compression. Equation (4) could be express in vector notation as,

$$\left[\frac{\partial \vec{V}}{\partial t} + \left(\vec{V}.\nabla\right)\vec{V}\right] = \vec{x} - \nabla P \qquad (5)$$

But by vector identity

$$\nabla\left(\vec{V}.\vec{V}\right) = 2\left(\vec{V}.\nabla\right)\vec{V} + 2\vec{V}\left(\nabla\vec{V}\right) \qquad (6)$$

By substitution in equation (5) it becomes

$$\rho\left[\frac{\partial \vec{V}}{\partial t} + \nabla\frac{V^2}{2} - \vec{V}\left(\nabla\vec{V}\right)\right] = \vec{x} - \nabla P \qquad (7)$$

Considering irrotational flow $\left(\nabla\vec{V} = 0\right)$, so equation (7) may be integrated . A velocity potential φ exist such that,

$$\vec{V} = -\nabla\varphi \qquad (8)$$

From the conservation of force fields, we have,

$$\vec{x} = -\nabla\Omega \qquad (9)$$

Thus,

$$\nabla\left(-\frac{\partial\varphi}{\partial t} + \frac{V^2}{2} + \frac{P}{\rho} + \Omega\right) = F(t) \qquad (10)$$

Where $F(t)$ is an arbitrary function of time. In the case of steady flow, with regard to gravity force $\left(\Omega = gz\right)$, where,

$$\frac{V^2}{2g} + \frac{P}{\rho g} + Z = Cte \qquad (11)$$

One is able to integrate equation (7) for inviscid rotational flow, and obtain equation (11). However, the constant will be different for each streamline.

The velocity potential φ satisfies Laplac's equation:

$$\nabla^2\varphi = 0 \qquad (12)$$

from the definition of φ and continuity it is known that $\vec{V} = -\nabla\varphi$ and $\nabla.\vec{V} = 0$.

In order to solve equation (12), φ is determined from equation (12) for the given boundary conditions, the velocity field is determined from equation (8) and pressure is deduced from the Bernoulli's equation. The design of probe to measure velocity is thus governed by the above equations.

However the occurrence of ideal uniform flow is very rare thus, measurement is often required in turbulent shear flow. Under these circumstances, it is convenient to measure total pressure with a total-head tube, and static pressure with a static head tube. The effect of the turbulence intensity for this measuring system is essentially due to the fact that the total probe senses total pressure, the instantaneous value being related to both velocity

and local static pressure. The total pressure sensed by the total tube is;

$$P_t = \frac{1}{2}\rho\left(\overline{U} + u'\right)^2 + \overline{P} + p' \qquad (13)$$

The time averaged value of equation (13) gives

$$\overline{P_t} - \overline{P} = \frac{1}{2}\rho\overline{U}^2 + \frac{1}{2}\rho\overline{u}'^2 \qquad (14)$$

Or

$$\frac{\overline{U}}{\left[\frac{2}{\rho}\left(\overline{P_t} - \overline{P}\right)\right]^{1/2}} = \left(1 + \frac{\overline{U}'^2}{\overline{U}^2}\right)^{1/2} = 1 - \frac{1}{2}\frac{\overline{u}'^2}{\overline{U}^2} + H.O.T \qquad (15)$$

Neglecting higher order terms, the mean velocity will be in error by 0.5% the square of the turbulent intensity when it is taken as;

$$\overline{U} = \sqrt{\frac{2}{\rho}\left(\overline{P_t} - \overline{P}\right)} \qquad (16)$$

There have been three methods introduced to evaluate the fluctuating part of the turbulent flow. The first was introduced by (Arndt and Ippen 1970), the other two methods are presented by (Mansoori 1988). Use of second and third methods depends on the kind of measurement system.

First Method: in this method an equation for the root mean square of turbulent velocity fluctuation is obtained by expanding equation (13)

$$P_t = \frac{1}{2}\rho\overline{U}^2 + \rho\overline{U}.u' + \frac{1}{2}\rho u'^2 + \overline{P} + p' \qquad (17)$$

Neglecting second order terms in equation (17) and taking the mean square, results in;

$$\sqrt{\overline{p'^2}} = \rho\overline{u}\sqrt{\overline{(u')^2}} \qquad (18)$$

Where

$$P' = P_t - \overline{P_t} \qquad (19)$$

And

$$\overline{P_t} = \frac{1}{2}\rho\overline{U}^2 + \frac{1}{2}\rho\overline{u'^2} + \overline{P} \qquad (20)$$

The third method by author where the two value of P'_t and p'_s are not time synchronized chosen for this study subtracting (20) from (17) yields,

$$P_t - \overline{P_t} = \rho\overline{U}u' + \frac{1}{2}\rho u'^2 - \frac{1}{2}\rho\overline{u'}^2 + p'_s$$

$$p'_t = \rho\overline{u}u' + \frac{1}{2}u'^2 - \frac{1}{2}\rho\overline{u'}^2 + p'_s \qquad (21)$$

Squaring equation (21) gives;

$$p'^2_t = \rho^2\overline{U}^2u'^2 + \frac{1}{4}\rho^2(u'^2)^2 + \frac{1}{4}\rho^2(\overline{u'^2})^2 + p'^2_s + \rho^2\overline{U}u'u'^2 - \rho^2U\overline{u'^2}u' + 2\rho\overline{U}u'p'_s - \frac{1}{2}\rho^2\overline{u'^2}\overline{u'^2} + \rho u'^2 p_s - \rho\overline{u'^2}p'_s$$

Hence,

$$\overline{p'^2_t} - \overline{p'^2_s} = \rho^2\overline{U}^2\overline{u'^2}$$

And finally the r.m.s value of the velocity fluctuation is given by;

$$\sqrt{\overline{u'^2}} = \frac{\sqrt{\overline{p'^2_t} - \overline{p'^2_s}}}{\rho\overline{U}} \qquad (22)$$

This method of calculation may be used when instantaneous values of the total and static pressure, at each position, are not measured individually, with the same time period, but not necessarily at the same time. Therefore, the pressure measurements were carried out longitudinally.

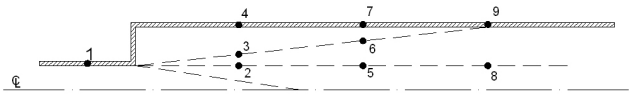

Fig. 1. Positioning of pressure measurements

Data was calculated at four longitudinal points in the flow, $x/D_j = -1, 2.15, 4.75$ *and* 7.36 at the latter three points measurements were taken across the flow at the center of fast moving eddies. At center line of diffusion zone, at the edge of the diffusion zone, and on the wall of the model (Fig. 1)

Graphs of the mean pressure, mean of the pressure data below mean pressure, and mean of the pressure data above mean pressure are shown for, center of fast moving eddies, the edge of the jet, and at the wall (Fig. 2, 3 and 4).

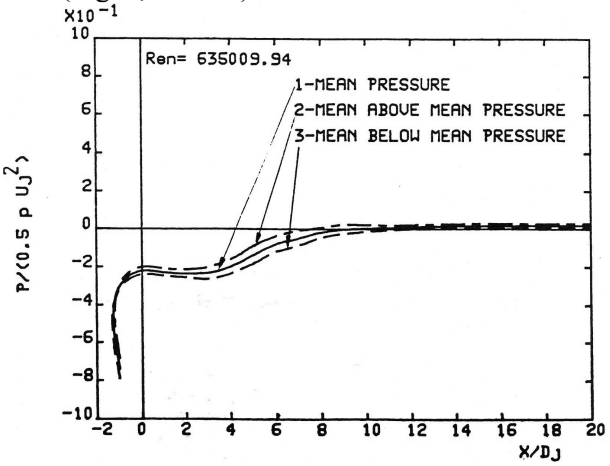

Fig. 2. Longitudinal distribution of mean wall-pressure, Re=635009.94

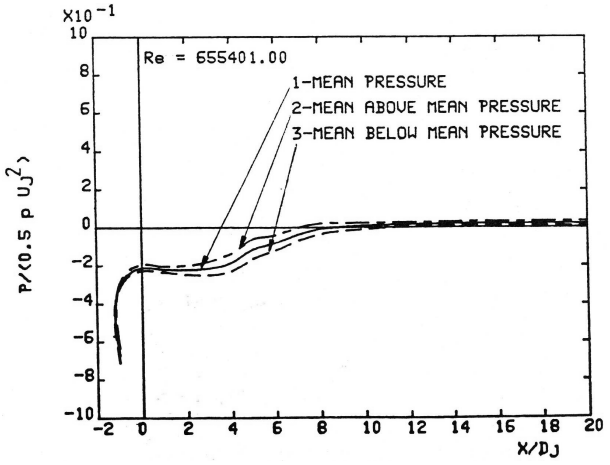

Fig. 3. Longitudinal distribution of mean wall-pressure, Re=655401.00

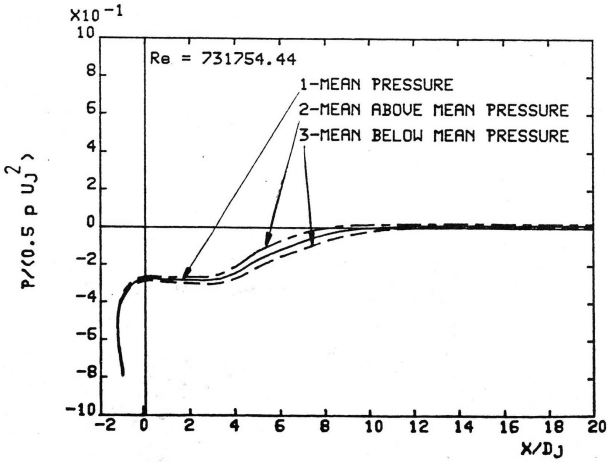

Fig. 4. Longitudinal distribution of mean wall-pressure, Re=731754.44

3 Experimental Apparatus

The apparatus used in this test is shown schematically in Fig. 5. The axisymmetric arrangement is of general application and it was more convenient for the purpose of this investigation.

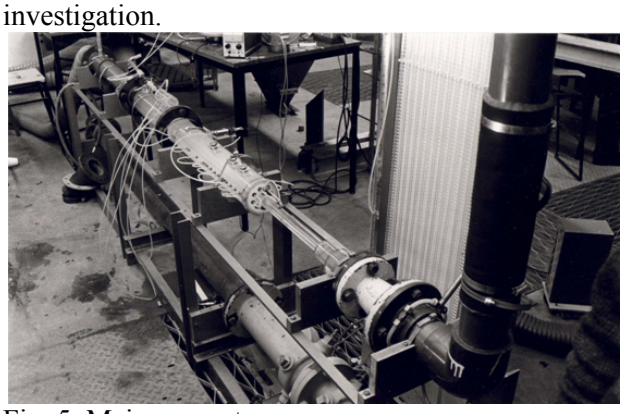

Fig. 5. Main apparatus

The larger of two main rings employed consisted of a smooth conical reducer leading to a 600mm long section of diameter, Dj=53mm. The expanded section was 138mm in diameter and 2400mm long; the whole being fabricated in transparent Perspex. Water entered the apparatus from a constant head tank 30m above the apparatus via a control valve.

Wall pressure tapings were located at distances $x/D_j = 0$ to 10, 15 and 20. The taping consisted of 10mm long copper tubes of bore 1.5mm flush mounted and sealed against the Perspex pipe with small "o" ring seals. One pressure transducer was used throughout. Data from the transducer was fed directly to a high-speed data logger controlled from a computer, acting as a terminal emulator for the data logger.

The data logger was programmed to acquire 480 readings in 24 second, because sensitivity studies had shown that this was the minimum sampling frequency and length record needed to define the required phenomena. The data sets were stored for subsequent analysis using a VAXA computer. Suitable programs, including a fast Fourier transform analysis to drive power spectra densities, were then applied to data.

4 Numerical Study

A two-dimensional flow of incompressible liquid (i.e. water) is considered. It expands from a straight pipe with diameter of Dj=53mm to a larger diameter of Dd=138mm. The length of these pipes are $600mm$ and $2400mm$, respectively (see Fig. 6). The wall-pressure variation in downstream pipe is desired.

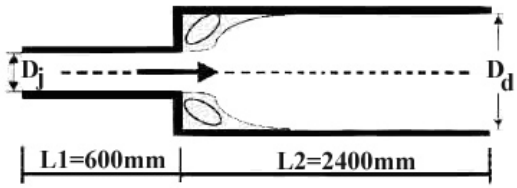

Fig. 6. Sketch of flow configuration

Mentioned problem has been studied by FLUENT V6.0 as a CFD code. this code the continuity and Navier-Stokes equations in their incompressible forms as governing equations. Different turbulence modeling schemes such as Spalart-Allmaras, Standard $k-\varepsilon$, RNG $k-\varepsilon$, realizable $k-\varepsilon$, standard $k-\omega$ and SST $k-\omega$ supported by this code. Description of the governing equations and other features of the code are presented by Karim (Karim 1996).

In order to obtain the wall-pressure variation, sudden expansion is simulated with various available one-equation and two-equation turbulent models. GAMBIT was used to define the geometry and structural grid of the problem. A quadrilateral computational mesh is mapped to the physical space of the problem. The grid information was then imported from GAMBIT to FLUENT. The physical models, fluid/material properties, and boundary conditions were next added to the grid information and stored in the case-file.

The imposed boundary conditions are obvious from fig.1: at the inlet ($x = -L_1$), a uniform velocity profile and at outlet ($x = L_2$) pressure outlet condition is assumed. At walls no slip conditions are imposed.

Considering the symmetry of the problem only one half of the geometry is investigated. To eliminate the effect of mesh size on the results, grids were made finer till the solutions be independent of grid size. Uniform distribution is assumed for inlet velocity. Pressure outlet boundary condition is specified for the flow outlet.

5 Results and discussions

A comparison between experimental and numerical results is shown in fig7 to 9. Six turbulent models have been run for sudden expansion ratio of 1:2.6. Spalart-Allmaras is used as a one-equation model. Realizable $k-\varepsilon$, RNG $k-\varepsilon$, Standard $k-\varepsilon$, SST $k-\omega$ and Standard $k-\omega$ are also used as two-equation models. The overall wall-pressure CFD-based predictions at all the flow rates have been examined. There are good agreements between numerical and experimental results.

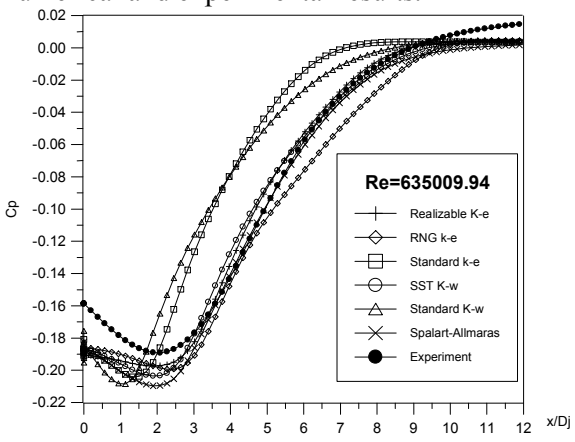

Fig. 7. Wall-Pressure variation for Re=635009.94

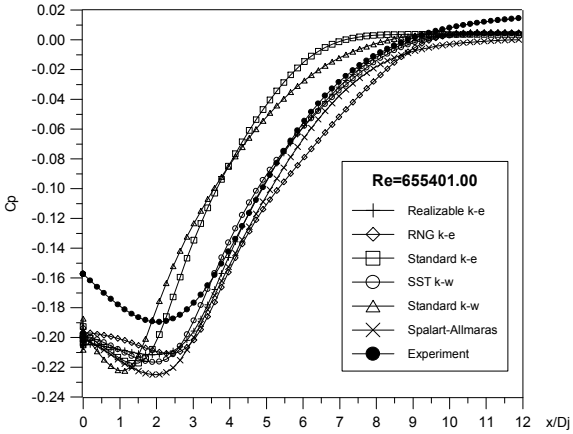

Fig. 8. Wall-Pressure variation for Re=655401.00

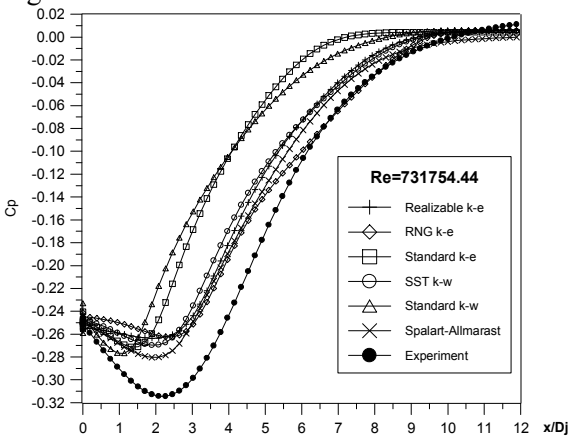

Fig. 9. Wall-Pressure variation for Re=731754.44

As it can be seen from figure 7 to 9 Spalart-Allmaras predictions for minimum wall-pressure are more conservative, so they can be a better choice for a safe design, using CFD. With respect to the computation cost, Spalart-Almaras model is better than the two-equation models mentioned above.

The evaluation of different turbulent models can be carried out from two different points of view. The first one is based on the value of minimum wall-pressure and its location. The second deals with the whole wall-pressure diagram and its agreement with experimental results.

In table 1 different models are ranked, based on the first point of view. The locations and values of minimum wall pressure for different models are summarized in this table. Ranking is based on location and value of minimum point of each curve in figures 7 to 9. Rank of 1 is assigned to the best match and rank of 6 is assigned to the worst match with experimental results. Summation of assigned ranks, determine the rank of a special model.

It can be seen that the Re=635009.94 and 655401.00 are very similar in ranking numbers. However, significant difference, especially in magnitude of minimum pressure ranking, is found for Re=731754.44. In general, if the location and

magnitude of minimum wall-pressure are of more interest, realizable $k-\varepsilon$ turbulent model is recommended.

Table 1. Location and magnitude of minimum below atmospheric pressure.

Re	$C_{p\,Minimum}$	Model	Realizable K-ε	RNG K-ε	Standard K-ε	SST K-ω	Standard K-ω	Spalart-Allmaras	Experiment
635010	Magnitude	**Value**	-0.19738	-0.19924	-0.20402	-0.20355	-0.2085	-0.2096	-0.18912
		Rank	**1**	**2**	**4**	**3**	**5**	**6**	-
	Location, (x/Dj)	**Value**	1.88679	2.2642	1.32075	1.88679	1.132075	1.886792	2.0755
		Rank	1	1	2	1	3	1	-
655401	Magnitude	**Value**	-0.21162	-0.2107	-0.21745	-0.2166	-0.22238	-0.22496	-0.18961
		Rank	**2**	**1**	**4**	**3**	**5**	**6**	-
	Location, (x/Dj)	**Value**	1.88679	2.45283	1.32075	1.88679	1.132075	1.88679	2.07547
		Rank	**1**	**2**	**3**	**1**	**4**	**1**	-
731754	Magnitude	**Value**	-0.26366	-0.26242	-0.27141	-0.26974	-0.27682	-0.28039	-0.31439
		Rank	**5**	**6**	**3**	**4**	**2**	**1**	-
	Location, (x/Dj)	**Value**	1.88679	2.45283	1.32075	1.88679	1.13208	1.88679	2.26415
		Rank	**2**	**1**	**3**	**2**	**4**	**2**	-

Table 2. Summation of squared distance of each CFD based curve shown in figure 7 through 9 to experimental curve.

Re	S_{d^2}	Realizable K-ε	RNG K-ε	Standard K-ε	SST K-ω	Standard K-ω	Spalart-Allmaras
635010	Value	0.030421	0.35176	0.97156	0.031991	0.094454	0.35285
	Rank	**1**	**3**	**6**	**2**	**5**	**4**
655401	Value	0.037856	0.044781	0.089937	0.037355	0.86137	0.055257
	Rank	**2**	**3**	**6**	**1**	**5**	**4**
731754	Value	0.037856	0.087643	0.387259	0.125732	0.399164	0.092195
	Rank	**2**	**1**	**5**	**4**	**6**	**2**

Table 3. Summation of ranking for each criterion

Summation of Rankings	*Real. K-ε*	*RNG K-ε*	*Stand. K-ε*	*SST K-ω*	*Stand. K-ω*	*S-A*
Due to magnitude	8	9	11	10	12	13
Due to Location	4	4	8	4	11	4
Due to Least Square	6	7	17	7	16	10
$\sum$	**18**	**20**	**36**	**21**	**39**	**27**

Table 2 is established, based on the second point of view. The deviation of each curve in figures 7 to 9 from experimental results is measured by least square method

The differences of ranks for different Reynolds numbers, which was shown in table 1, can be seen in table 2.

Summation of rankings for each criterion is shown in table 3. There are three criteria for making decision about the best method. The modeler can make decision by assigning his/her desired weight to each criterion and select the best by the weighted summation. If the same weights are assigned to all criteria, then a simple summation shows that Realizable $k-\varepsilon$ is the best model. Other methods of weightings may put other models in the first rank.

4 Conclusions

Flow with high Reynolds number in a pipe with sudden expansion causes wall negative pressure near the expanded area. The nature of wall-pressure at high Reynolds numbers is stochastic due to fluctuation. These fluctuations make the problem analysis and modeling more complex. There is still a challenge in modeling such uncertain phenomena; therefore experiment is the best tool in modeling development and verification. Because of experimental cost and scaling problem, numerical modeling attracts more attention. However, modelers have to choose the proper turbulent model as the first step of each numerical modeling task.

In this paper two different view points are considered in ranking different mentioned turbulent models. The first one uses the maximum negative wall-pressure value and its location as criteria for ranking. The other one, consider the whole wall pressure diagram instead of focusing on minimum point of the curve. Each view point leads to a rank for turbulent models. Combining these ranks with different weight may develop a new rank. If two mentioned view points have the same contribution, Realizable $k-\varepsilon$ is the best. Considering the differences between ranks, turbulent models can be categorized into accurate and inaccurate models. Accurate models include Realizable $k-\varepsilon$, RNG $k-\varepsilon$ and SST $k-\omega$ and inaccurate ones include Spalart-Allmaras, Standard $k-\varepsilon$ and Standard $k-\omega$. This work shows the workhorse of practical engineering flow calculation, standard $k-\varepsilon$, lies in inaccurate category for modeling sudden expansion flow.

5 Acknowledgement

Contribution of Dr. Sayyed Mohammad Binesh and Dr. Akbar Karimi, Faculties of civil engineering department of Islamic Azad University-East Tehran branch, in revising this paper are hereby acknowledged.

6 Notations

The following symbols of are used in this paper:

u	stream wise velocity
x_i	components of the body force field
τ	shear stress
T	time
D	denote full differentiation
P	pressure
∇	gradient
V	velocity
ρ	density
φ	velocity potential
Ω	=gz
u’	turbulent velocity in x direction
$\overline{p}$	mean pressure
P_t	total pressure
P’	fluctuating pressure
$\overline{U}$	mean velocity
L	pipe length
D_d	downstream pipe diameter
D_j	jet diameter
x	Streamwise distance from expansion
Re	Reynold’s number
U_j	jet velocity
Cp	pressure coefficient ($C_p = p/0.5\rho u_j^2$)
S_{d^2}	Summation of squared distance to experimental curve
δ	denote partial differentiation

7 References

[1] Arndt, R.E. and Ippen, A.T. (1970). Turbulence measurement in liquid using an improved total pressure probe*, Journal of Hydraulic research,* Vol.8, No.2.

[2] Back, L.H. and Roschke, E.J. (1972). Shear-Layer Flow Regimes and Wave Instabilities and Reattachment Lengths Downstream of an Abrupt Circular Channel Expansion, Transactions of the ASME, J. Applied Mechanics, 39, pp. 677-681.

[3] Chaturvedi, M. C. (1963). Flow characteristics of axisymmetric Expansions, Journal of Hydraulic Division, ASCE, Vol89, No. HY3.

[4] Johnston, J.P. (1976). *Internal Flows, Turbulence. Topics in Applied Physics*, Springer Verlag.

[5] Karim, O. A. (1996). Prediction of two and three dimensional turbulent flows, *Ph.D. thesis, University of Liverpool*.

[6] Mansoori A., and Sabouri F. (2004). Determination of Scour due to analysis of turbulent jets, *Journal of faculty of Engineering(Civil Engineering)*, Tabriz university press, Vol30, No. 3

[7] Mansoori, A. (1988). The flow characteristics of a bounded jet sudden enlargement including the phenomena of cavitation", *Ph.D. dissertation, King's college, London university.*

[8] Moon, L.F. and Rudinger, G. (1977). Velocity Distribution in an Abruptly Expanding Circular Duct. *ASME J. Fluids Engineering*, 99 pp. 226-230.

[9] Poole, R.J., Escudier, M.P. (2004). Turbulent flow of viscoelastic liquids through an axisymmetric sudden expansion, *J. Non-Newtonian Fluid mech.*, 117, pp 25-46.

[10] Rouse H., and Jezdinsky, V. (1966). Fluctuation of pressure in conduit expansion, *Journal of hydraulic Devision*, ASCE, HY3.

[11] Stieglmeier, M., Tropea, C., Weiser, N and Nitsche, W. (1989). Experimental Investigation of the Flow Through Axisymmetric Expansions. ASME, *J Fluids Engineering*, 111, pp. 464-471.

[12] Sullivan, P.E. and Glauser, M.N. (1990). An Experimental and Numerical Investigation of a Sudden Expansion, Report Number MAE-216, Clarkson University.

[13] Szczepura, R.T. (1985). Flow Characteristics of An Axisymmetric Sudden Pipe Expansion; Results Obtained From the Turbulent Studies Rig, Part 1; Mean and Turbulence Velocity Results. Technical Report TPRD/B/0702/N85 Central. Electricity Generating Board, Berkeley Nuclear Laboratories, England.

[14] FLUENT 6.0 User's Guide, Fluent Inc. Press, 2001